



**Metal Nanoparticles-Semiconductor Nanowire Hybrid
Nanostructures for Plasmon-enhanced Optoelectronics and
Sensing**

Journal:	<i>Journal of Materials Chemistry C</i>
Manuscript ID	TC-REV-06-2015-001820.R1
Article Type:	Review Article
Date Submitted by the Author:	08-Sep-2015
Complete List of Authors:	Pescaglini, Andrea; University College Cork, Tyndall National Institute Iacopino, Daniela; Tyndal,

Metal Nanoparticles-Semiconductor Nanowire Hybrid Nanostructures for Plasmon-enhanced Optoelectronics and Sensing

Andrea Pescaglini and Daniela Iacopino*

Received Xth XXXXXXXXXXXX 20XX, Accepted Xth XXXXXXXXXXXX 20XX

First published on the web Xth XXXXXXXXXXXX 200X

DOI: 10.1039/b000000x

Plasmonic metal nanoparticles have recently attracted increasing interest due to their nanosized dimensions, tunable optical properties in the visible and near-infrared region of the spectrum and easy manufacturing. Although the optical properties of these sub-wavelength objects arising from plasmonic resonances have been extensively investigated in both isolated and assembled structures, their rational integration in 1D semiconductor-based devices for generation of engineered properties is a novel and vastly unexplored field. In particular, development of metal nanoparticle-1D semiconductor hybrid nanostructures has been hampered by a number of challenges including limited control of component assembly processes and modest theoretical and experimental understanding of fundamental physical phenomena occurring in such hybrids. In this feature article we describe recent progress in fabrication methods and we review the relevant plasmonic properties of metal nanoparticles that can be exploited to manipulate, enhance and optimize the performances of semiconductor nanowire-based devices. Finally, we explore the enhanced properties of hybrid metal nanoparticle-semiconductor nanowire structures and describe their application in optoelectronics and sensing.

1 Introduction

In the last decades we have assisted to a progressive miniaturization of electrical components, driven by the semiconductor industry, towards the fabrication of more compact, low-power consumption and faster portable electronic devices. From a technological point of view, the miniaturization process needs to be supported by progresses in CMOS-compatible fabrication techniques, in order to reach higher resolutions (~ 15 nm for state-of-the-art transistors). Additionally, a deeper understanding of the electronic properties of semiconductor materials and low-dimensional systems with a size-regime approaching the border line between classical and quantum mechanics is also an essential requirement towards further miniaturization.

The nano-sizing evolution in the semiconductor electronic field, described by the well-known Moore's law, is actually able to realize truly nanoscale elements fully capable to compute, transmit and store data. As discussed, further improvement in performance are linked with the ability to increase the density of the operational units, achievable by reducing the size of transistors, as well as the speed at which data are computed and transmitted. Regarding the former aspect, the present technology is still capable of further improvement in terms of resolution and device densities, although accessing quantum regime paradigm will require completely novel tech-

nologies and architectures for computing data, as assessed by the emerging research field of quantum information and computation.¹ On the other hand, processor performances in semiconductor technology show limitations. Heat generation and signal delay issues associated with electronic interconnection limit the speed rate to a range of ~ 10 GHz.² Consequently, further improvement directed to exceed such range will require the development of radically new chip-scale technology able to operate beyond the limits imposed by semiconductor technology and to reach optical frequencies that, to date, are only achievable in dielectric photonics (Fig. 1).³ Unfortunately, photonic circuitry cannot be easily scaled below the diffraction limit of the light (about $\sim \lambda/2$ that is one to two orders of magnitude larger than the electronic counterparts), therefore the large mismatch between electronic and photonic components has up to now hampered the on-chip integration and miniaturization.

The new flourishing field of technology called *Plasmonics*, has recently emerged as a potential route towards miniaturization of optical components beyond the limit of traditional optics.^{4,5} This capability is made possible by exploiting coherent electron excitations in the electronic gas of metal nanostructures and their ability to manipulate, propagate and enhance light in nanoscale volumes.⁶ When metallic atoms form a crystal structure, valence electrons are shared in orbitals delocalized on the entire crystal and acquire a quasi-free nature.⁷ Application of Maxwell's equations at the metal-dielectric interface result in propagating wave-like solutions, also called

^a Tyndall National Institute-UCC, Dyke Parade, Cork, Ireland. E-mail: andrea.pescaglini@tyndall.ie

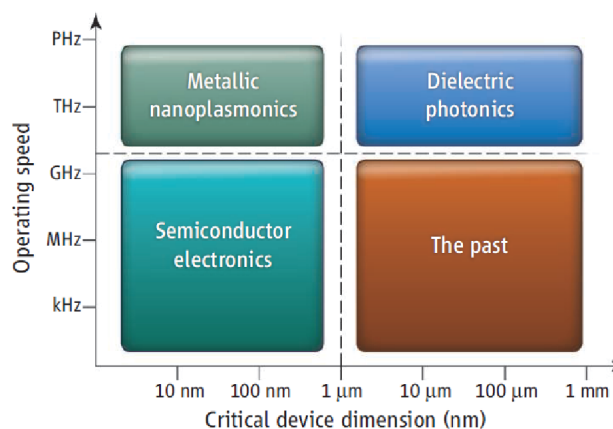


Fig. 1 Characteristic domains in terms of operating speed and device sizes for semiconductor (electronics), dielectrics (photonics) and metals (plasmonics). Adapted with permission.² Copyright 2010, AAAS

surface plasmon polariton (SPP). The distinctive characteristic of surface plasmons compared to photons is that they have much smaller wavelength at a given frequency.⁸ Therefore, using SPP enables the fabrication of nanoscale optical integrated circuits in which light can be guided, split, filtered, focused and also amplified in plasmonic nanodevices smaller than the optical wavelength.^{9,10} For metallic nanostructures significantly smaller than the free-space wavelength, geometrical boundary conditions determine the frequency at which the electron oscillation are driven resonantly (in this context called *localized surface plasmon*) producing a very strong charge displacement and high field intensity in close proximity to the nanostructure (typically within 15 nm).¹¹ From this fundamental mechanism derive the unique optical properties and an extraordinary ability to concentrate light into sub-wavelength volumes and mediate, enhance the interaction between the propagating radiation and nanoscale objects.^{6,12}

On the other hand, in semiconductor technology the attempt to further reduce the size of active components has focused increasing attentions in fabrication routes and fundamental properties of 1D semiconductor nanowires. Growth techniques, based on vapour-liquid-solid (VLS) mechanism, have allowed fabrication of a broad range of inorganic nanowire compositions such as Si, Ge, ZnO, CdS, GaN, GaAs, InP, InAs and also traditional less accessible compositions like InGaN,^{13–16} as well as axial and radial heterostructured nanowires accommodating large lattice mismatches with unprecedented level of flexibility in material engineering.¹⁷

Recently, integration of metal nanoparticles into semiconductor nanowires has been shown as a viable route for the expansion and enhancement of nanowire functionalities.^{18–20} In

fact, hybrid architectures combine the strength of both fields: plasmonic active nanoparticles can be integrated to enhance, expand and tune the light interaction with semiconductor component; at the same time, homogeneous or heterostructured semiconductor 1D materials can be realized to offer the optimum optical and/or electrical properties required in operational devices. Overall, the degree of freedom in design and optimization afforded in a single hybrid nanostructure opens up an exciting and novel field of research still vastly unexplored.

In this review article we first present the techniques explored to fabricate hybrid metal nanoparticles-semiconductor nanowire (HbNW) nanostructures. In section 3 we discuss some of the most remarkable properties of nanowire-based optoelectronic and sensing devices achievable by exploring the 1D nature and the composition versatility of nanowires combined with the plasmonic features of metal nanoparticles. Great emphasis will be placed on the plasmonic-related processes and properties of metal nanoparticles that can be manipulated and exploited to add additional or improved capabilities to semiconductor nanowires. In particular, two different plasmonic-related processes will be discussed: the electric field enhancement in close proximity to the metal surface, responsible for enhancing light-matter interaction (such as light absorption, SERS and non-linear optical processes) and the generation of energetic electron-hole pairs that plays a crucial role in all processes involving photon-electron conversion (such as photodetection, solar cell and catalysis). Finally in section 4 relevant applications of HbNWs in photodetection, photovoltaics and molecular sensing will be presented.

2 Fabrication methods : from single components to hybrid 1D nanostructures

A well known approach to load metal nanoparticles on the surface of nanowires is sputtering deposition (see Fig. 2a).^{21–23} This technique forms nanoparticles with size below ~ 10 nm and is very attractive due to its simplicity, reliability and relative low-cost. Particle density can be moderately adjusted by changing the process conditions (sputtering current, distance to the target substrate) and the deposition time.²⁴ The absence of any stabilizing chemical agents during the deposition ensures an extremely clean process with the metal surface in direct contact with the semiconductor. Atomic layer deposition (ALD) is also a viable method for decorating semiconductor nanowires with noble metal nanoparticles.²⁵ Although this technique is often used for the conformal growth of thin films with atomic control on thicknesses and composition, aggregation instead of uniform coating can be obtained for an appropriate precursor-substrate combination where the homogeneous chemical adsorption of precursors at the substrate

surface is inhibited.²⁶ This is the case of noble metal ALD on oxide surfaces, where at early stage the nucleation in localized spots results in nanoparticle formation.^{27,28} A major drawback of sputtering and ALD is that only quasi-spherical shapes can be achieved and increasing deposition times lead to uncontrolled aggregation and eventually formation of continuous films.

For nanowires with large enough diameter, top-down fabrication (e-beam lithography) becomes a possible technique to fabricate geometry-customizable metal nanostructures directly on the nanowire²⁹ or in its proximity³⁰ within the resolution of the lithographic process (see Fig. 2b-c). However, top-down fabrication of metal nanostructures is not exempt from limitations. The resolution of the lithography process (~ 20 nm) prevents investigation of metal nanostructure behavior in the quantum regime (sub-10 nm sized structures)³¹ and of enhancing phenomena in arrays with inter-particle distance below 10 nm (strongly-coupled regime), interesting for catalysis, quantum optics and sensing.³² Other drawbacks include the polycrystallinity of the nanostructures, the presence of an additional layer required to ensure the adhesion to the substrate (usually titanium or chromium) and prohibitive costs that prevent any integration into commercial devices.

Bottom-up synthetic approaches constitute valid alternatives as they address most of the limitations of top-down techniques. Among them, galvanic displacement was used to decorate Si nanowires with Au and Pt nanoparticles of different morphologies.^{33,34} In this process the nanowire provided electrons for reduction of metal ions in solution and at the same time served as template for the particles formation. Typical nanostructures resulting from the process are shown in Fig. 2d-e. Different particle shapes were synthesized (spherical, triangular, rod-like) with diameter between 20-100 nm attached to the nanowire body with less than 1 nm distance from the nanowire surface. Site-specific growth of Ag nanoparticles located at the ends of ZnO nanorods was demonstrated by photodeposition.³⁵ In this approach optically excited electrons in the semiconductor conduction band reduced metal ions in solution leading to a metal atom deposition and self-organization into spherical shape. The crystal planes with reduced lattice mismatch between ZnO and Ag located at the ends of the nanorod determined the most favorable site for particle nucleation. A similar mechanism was also proposed to explain the formation of Ag nanorods and spheres during vapor-solid growth of ZnO nanowires on a silicon substrate covered by Ag nanoparticles.³⁶

An alternative method consists into drop-casting of chemically synthesized colloidal nanoparticles directly on the nanowire.^{37,38} In this approach an hosting substrate with nanowires deposited on the surface is covered by a droplet of the colloidal solution and after solvent evaporation a random deposition of nanoparticle homogeneously distributed on the

substrate is obtained. Figure 2f shows the result of this process on a Si nanowire deposited on Si/SiO₂ substrate contacted with two Al electrodes. Despite the simplicity of the process, its effectiveness was limited, as demonstrated by the small number of particles decorating the nanowire and the relative random location. Moreover, coffee-stain effects during solvent evaporation induced preferential nanoparticle accumulation at the border of the droplet, greatly reducing the density of particles deposited on the remaining substrate surface.³⁹ Also capillary effects during solvent evaporation drove particle deposition at the nanowire-substrate contact points, preventing efficient coverage of the actual nanowire surface (particularly in nanowires with diameter much larger than the particle diameter).

Some of these limitations were addressed by the mask-selective droplet deposition method, recently developed in our group.⁴⁰ In this method nanowires were deposited on a host substrate and a layer of photoresist was used as an effective mask to selectively expose the nanowire top surface to air. Following the droplet deposition of colloidal nanoparticles the photoresist was removed, leaving only nanoparticles attached on the exposed surface of the nanowire. A representative image of Au nanorods-decorated ZnO nanowire hybrid nanostructures is shown in Fig. 2g, depicting high yield deposition of Au nanorods preferentially deposited on the nanowire surface. The main advantage of droplet deposition methods relies in the ability to decouple the nanoparticle formation from the deposition step. The nanoparticle size and shape can be finely tuned by synthetic methods prior deposition⁴¹⁻⁴⁶ and nanowires can be homogeneously decorated with nanostructures having a specific geometry.

Finally, we also mention that attachment of Au colloidal nanorods onto ZnO nanowires was also demonstrated by chemical functionalization with poly(2-vinyl pyridine) (Fig. 2h-i).⁴⁷ This is a very promising approach because it allows an effective coverage of the nanowire surface for both isolated nanowires and vertical arrays, although this chemical functionalization process may not be readily extended to other materials different from ZnO.

Overall, simultaneous control of particle shape, size and location on the semiconductor nanowire component remains a key challenge and constitutes the major bottleneck for the realization of plasmonic hybrid devices by design.

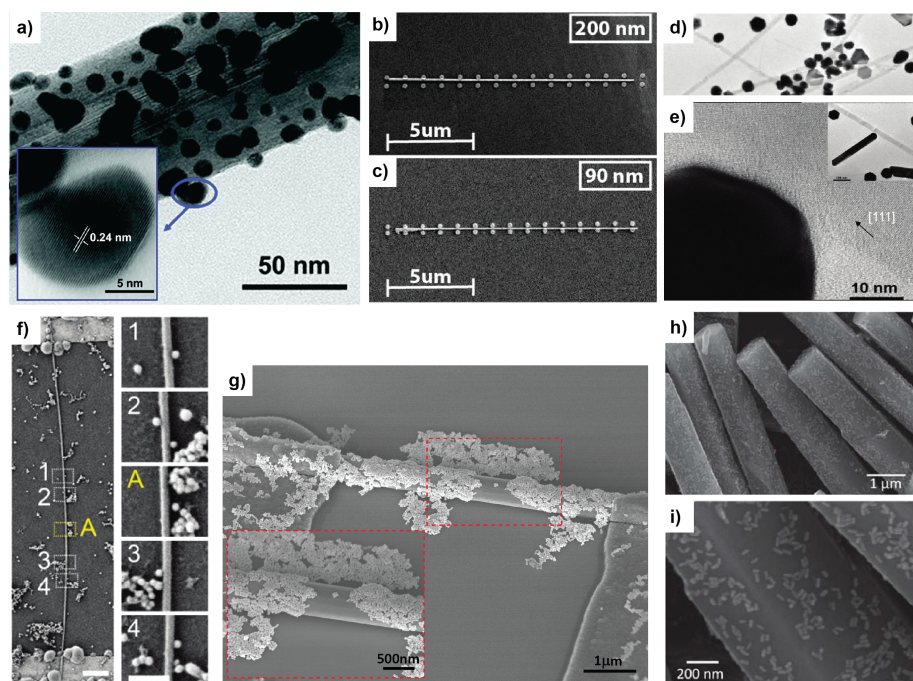


Fig. 2 Hybrid metal nanostructures decorated semiconductor nanowires obtained by a) sputtering technique,⁴⁸ b)-c) e-beam lithography,³⁰ d)-e) galvanic displacement,³³ f) droplet deposition,³⁷ g) mask-selective droplet deposition,⁴⁰ and h)-i) chemical functionalization.⁴⁷ Adapted with permission from a) Copyright 2015, RSC; b)-c) Copyright 2014, ACS; d)-e) Copyright 2012, ACS; f) Copyright 2011, ACS; g) Copyright 2014, ACS; h)-i) Copyright 2011, RSC.

3 Properties of hybrid nanostructure: semiconductor nanowires and metal nanoparticles

3.1 Semiconductor nanowires for photonic and sensing applications

The 1D nature of semiconductor nanowires together with dislocation-free structure and the ability to accommodate large lattice mismatch are associated with a number of properties interesting for nanoelectronic and photonic applications.^{49,50}

For instance, in photodetection, semiconductor nanowires have showed great potential due to (i) the prolonged lifetime of photogenerated carriers mediated by the in-built radial potential promoted by surface states and (ii) the reduced carrier transit time due to the high mobility achievable in high-quality single-crystal material combined with micrometer or nanometer inter-electrodes distance. In 2001 Lieber's group presented one of the first examples of single InP nanowire photodetector exhibiting highly polarized photoluminescence and polarized-sensitive photoconductivity with responsivities of 3000 A/W.⁵⁷ Following this pioneering work many other materials were explored such as GaN, Si, Ge, Se, CdS, ZnO among others.⁵⁸ For instance, Soci *et al.* realized a single-

crystal ZnO nanowire UV photodetector with photoconductive gain up to 10^8 (Fig. 3a).⁵¹

Moreover, careful design of the nanowire geometry was found capable to boost device performances. Brongersma *et al.* showed that light absorption in nanowires can be engineered by exploiting internal leaky modes resonances in optimized geometries (Fig. 3b). The authors demonstrated a 25-fold enhancement in the absorption and wavelength selectivity in Ge nanowire due to structural engineering.⁵² This approach was applied to other semiconductor nanowires and allowed to boost the optical absorption beyond the intrinsic properties of the material.⁵⁹

Nanowire properties explored for photodetection are equally relevant for designing nanowire-based solar cells. To this aim both radial and axial heterostructured nanowires have been proposed.⁶⁰ For instance, Tian *et al.* realized a single p-type/intrinsic/n-type (p-i-n) coaxial silicon nanowire solar cell.⁵³ In this geometry the electron-hole pairs generated under radiation in the intrinsic part were readily collected at the p-type core and n-type shell thanks to a carrier collection distance smaller than the minority carrier diffusion length (Fig. 3c). This efficient carrier collection scheme allowed to reach an overall apparent efficiency of 3.4%. Using a similar radial structure, higher efficiency up to 4.5% was demonstrated

in GaAs nanowires under comparable illumination conditions (1.5 AM).⁶¹ Substantial improvement in light absorption was obtained in vertical arrays of axial p-i-n InP nanowires with optimized diameter size and length of the top n-segment, demonstrating a record efficiency of 13.8 %, comparable to planar InP cells (Fig. 3d).⁵⁴ Despite the variety of alternative materials^{62,63} and geometries explored,^{58,60} the limited efficiency observed in semiconductor nanowire solar cells and photodetectors was mostly attributed to the limited light absorption caused by the sub-wavelength dimensions.⁶⁴

The 1D geometry, high refractive index, high crystal quality and adjustable diameter and length dimensions make nanowires natural optical gaining media for nanolasers and LEDs. Fabry-Perot waveguide modes tunable with the nanowire length⁶⁵ were observed in a number of optically pumped binary semiconductors (see Fig. 3e) such as ZnO,⁶⁶ CdS,^{55,67} and GaN⁶⁸ with quantum efficiencies up to 60%.⁶⁹ Additionally, rational design of heterostructured nanowires containing multi-quantum-wells,^{70,71} self-assembled quantum dots,^{72,73} and band-graded materials^{74–77} acting as gaining media inside the nanowire optical cavity have been explored for wavelength-tunable nanolaser and proposed as building blocks for light-emitting devices. Also, electrically injected nanolasers based on single nanowires^{78,79} and arrays^{56,80} have been successfully demonstrated opening up attractive perspectives for intra-chip optical interconnection applications (see Fig. 3f).⁸¹

Finally, we mention that the large surface-to-volume ratio in nanowires offers obvious advantages for molecular and gas sensing. In fact, following the same principle of field-effect transistors where a voltage applied to a channel gate results in a modulation of the channel conductivity, molecules adsorbed on a nanowire surface change the surface band bending and consequently the nanowire electrical transport properties (see Fig. 4a). Therefore nanowires represent a very promising tool for sensitive detection of target molecules via electrical readout. To this aim different geometries, mechanism and materials were explored. ZnO nanowires were largely used for gas sensing due to the low fabrication cost and high sensitivity to gases such as O₂,^{82,83} NO₂,⁸⁴ ethanol,⁸⁵ H₂S,⁸⁶ and NH₃.⁸⁷ In addition sensing properties of ZnO were enhanced via higher working temperature,⁸⁵ piezotronic effect,^{88,89} polymer functionalization^{90,91} and defects concentration.⁹² An interesting scheme to enhance the sensitivity of up to 5 orders consisted in introduction of a non-symmetrical Schottky contact between metal and nanowire.^{93,94} In this scheme the device contained an Ohmic contact and a Schottky barrier contact where the barrier height, and consequently the current passing through the device in reverse bias condition, resulted extremely sensitive to the interaction with the surrounding medium (i.e. adsorbed biomolecules, gases and light irradiation), as showed in Fig. 4b-c. Follow-

ing the same principle, interdigitated nanowire architectures were explored to increase the gas sensitivity by exploiting the Schottky-to-Schottky double barrier at the interface between two nanowires.⁹⁵ Nanowire field-effect transistors were also shown capable of detecting molecules with concentrations in the range of pM that was further lowered to ~1.5 fM using the device in subthreshold regime.⁹⁶ Air-bridge contacted vertical arrays of InAs nanowires displayed increased sensitivity due to the exposition of the entire nanowire surface to the analyte (see Fig. 4d-e).⁹⁷ This approach together with the electron accumulation layer at the InAs surface, resulted in sensitivity to NO₂ at parts-per-billion level. An alternative mechanism exploited the sharp metal-insulator phase transition of VO₂ at which the nanowire conductivity increased of several orders of magnitude, leading to successful detection of chemically inert and reactive gases.⁹⁸ Despite demonstration of ultra-low detection limits achievable with nanowire-based sensors, the major challenge in this field remains selectivity. In fact the high sensitivity due to the large surface-to-volume ratio can result in the impossibility of distinguishing individual contributions in real environments where more than one type of molecule interacts with the nanowire. This brief snapshot on the main photonic and sensing capabilities of semiconductor nanowires demonstrates the large potential of 1D nanostructures for technology development. However, nanowires are not exempt from limitations. In section 4 we will show how integration of metal nanoparticles with semiconductor nanowires can solve some of these limitations providing better performance in these application fields.

3.2 Plasmonic properties of metal nanoparticles: theory and design

The plasmonic properties of metal nanoparticles simply arise from the negative sign of the dielectric function at visible frequencies. This behavior gives rise to plasmonic resonant oscillations that generate an intense dipole-like electromagnetic field rapidly decaying outside the metal and to excitation of electron-hole pairs via non-radiative plasmon decay. The energy at which these processes occur can be easily tuned by modification of the shape, size and local environment of the metal nanoparticle. modify the metal response by increasing the absorption already in the visible range of the spectrum (Fig. ??).

3.2.1 Plasmonic-enhanced electromagnetic field

When the electron gas is confined in volumes $V \ll \lambda^3$ the plasma experiences a nearly space-independent external field (*quasi-static approximation*) and modes arise naturally from the solution of Laplace equation $\nabla^2\Phi = 0$ with Φ the electrical potential. Due to their non-propagating nature, these modes are known as *localized surface plasmons*. The oscillating electronic system leads to resonances that amplify the field

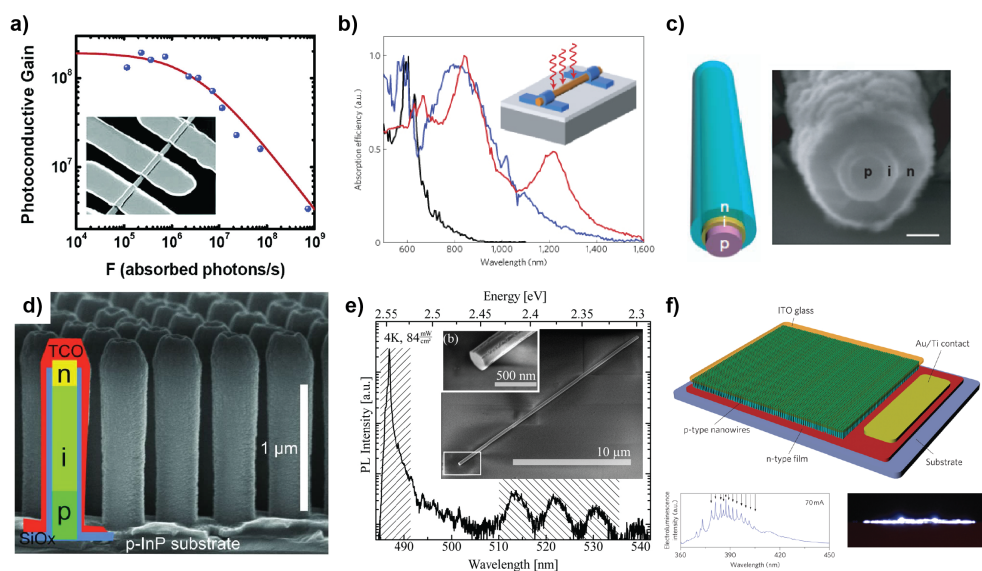


Fig. 3 a) Photoconductive gain versus photon absorption rate in ZnO nanowire photodetectors irradiated with light wavelength at 390 nm. Inset shows the scanning electron microscopy (SEM) image of the device.⁵¹ b) Measured spectra of the absorption efficiency Q_{abs} under unpolarized light taken from individual Ge nanowires with radii of 10 nm (black), 25 nm (blue) and 110 nm (red). Inset depicts a schematic illustration of the device.⁵² c) Schematic of a single core-shell Si nanowire solar cell and the SEM image of the nanowire cross section.⁵³ d) SEM image of a vertical InP nanowire array solar cell with superimposed the p-i-n doping levels.⁵⁴ e) Microphotoluminescence spectrum of a single CdS:Sn nanowire nanolaser at 4 K optically pumped at 325 nm showing near band edge emission (485–491 nm) and the donor-acceptor pair transition and the LO phonon replica (510–540 nm).⁵⁵ f) Schematic of an electrically pumped ZnO nanowire array laser device and the electroluminescence spectrum of the device operating at 70 mA with the related side-view optical microscope image.⁵⁶ Adapted with permission from a) Copyright 2007, ACS; b) Copyright 2010, ACS; c) Copyright 2007, NPG; d) Copyright 2013, AAAS; e) Copyright 2013, ACS; f) Copyright 2011, NPG.

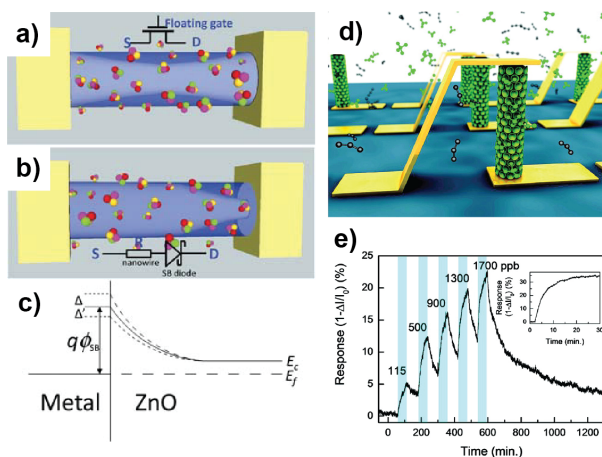


Fig. 4 Schematic of the working principle of a) field-effect sensing mechanism and b) the Schottky-gated device. c) Energy-band diagram of the metal-ZnO Schottky contact.⁹³ d) Illustration of InAs vertical nanowire array sensor and e) the response (percentage of the current variation) of an array of 200 nanowires to varying concentration of NO_2 in N_2 . The inset shows the time response to 9 ppm.⁹⁷ Adapted with permission from a)-c) Copyright 2010, WILEY-VCH Verlag GmbH & Co. KGaA; d)-e) Copyright 2010, ACS.

both inside and in the near-field zone outside the metal nanostructure. Another interesting consequence of the confinement to nanoscale volumes is the possibility to excite directly the surface plasmons without phase-matching techniques that are instead required for volume plasmons and SPPs.

For the highly-symmetric geometry of an homogeneous sphere in a non-absorbing medium with dielectric function ϵ_m the spatial electric field distribution can be easily calculated analytically. The polarizability experiences a resonance enhancement in correspondence to the minimum of $|\epsilon(\omega) + 2\epsilon_m|$, corresponding to⁹⁹

$$\text{Re}[\epsilon(\omega)] = -2\epsilon_m \quad (1)$$

that is called *Fröhlich condition* and the associated mode the *dipole surface plasmon*. In a free electron plasma, the eq.(1) is verified at the frequency ω_{isp} defined by

$$\omega_{isp} = \frac{\omega_p}{\sqrt{1 + 2\epsilon_m}} \quad (2)$$

where n is the number density of electrons, ϵ_0 the permittivity of the free space, m_e the electron effective mass and $\omega_p^2 = ne^2/\epsilon_0 m_e$ is the *plasma frequency* of the free electron gas. This relation shows that the localized surface plasmon frequency is always smaller than the plasma frequency and, most importantly, it is affected by the dielectric constant ϵ_m of the surrounding medium. The latter property in particular is

of great interest for sensing applications since the presence of a target molecule in the medium or its binding event on a receptor can change ϵ_m and therefore be detected via monitoring ω_{isp} (see also section 4.2).

The total electric field associated with the oscillating electronic gas in the near-field zone shows a fast spatial decay $\sim r^{-3}$ in proximity of the metal surface. Such a strong damping limits the volume where a molecule can be located in order to experience the plasmonic-mediated enhancement of the optical properties. On the other hand, at large distance from the metal nanostructure the dipole radiation is well approximated by a spherical wave, with the typical $\sim r^{-1}$ decay.¹⁰⁰

In the case of a metal nanostructure with the more general ellipsoidal geometry, with semiaxes $a_1 \leq a_2 \leq a_3$, Gans formulation¹⁰¹ of the analytical solution for the Laplace equation leads to multiple plasmonic resonances at frequencies solution of

$$\text{Re}[3\epsilon_m + 3L_i(\epsilon(\omega) - \epsilon_m)] = 0 \quad (3)$$

where L_i is the depolarizing factor for the axes $i=x,y,z$.¹⁰² Using the dielectric function for an ideal free electron gas we arrive to the expression of the localized surface plasmon resonance frequencies

$$\omega_{isp,v} = \omega_p \sqrt{\frac{1}{1 + \epsilon_m \frac{1-L_v}{L_v}}} \quad (4)$$

Within the class of ellipsoids, spheroids with $a_1 = a_2 < a_3$ are particularly interesting because they represent a reasonable approximation to the real geometry of chemically prepared rod-shaped metal nanoparticles. For these non-spherical nanoparticles the polarizability exhibits two spectrally separated plasmon resonances, corresponding to the oscillation of the electron plasma along the long (\parallel) and short (\perp) axes, therefore since $L_{\parallel} < L_{\perp} < 1$, we have the following relation between the two frequencies $\omega_{isp}^{\parallel} \leq \omega_{isp}^{\perp}$. Finally, we observe that the analytical solution of the Maxwell's equations can be obtained only in these simple geometries. Solving the equations for a generic non-spherical particle requires numerical methods such as discrete dipole approximation,^{103,104} boundary element methods^{105,106} and finite difference time domain methods.¹⁰⁷

3.2.2 Plasmonic-mediated hot electron generation

The local re-radiation of the incident electromagnetic field discussed in the previous section has been extensively investigated for mediating the light interaction with single emitters and for taking advantage from the double effect of enhancing the incident radiation and the light scattered off from the object.¹⁰⁸ In this process the radiative decay of the excited plasmon by re-emission of a photon (related to the scattering cross section) needs to be more effective of the non-radiative

decay (related to the absorption cross section) where the incident photon energy is *lost* in non-radiative transition and eventually converted into heat.¹⁰⁹

Recently, the non-radiative decay process has attracted considerable interest motivated by the possibility to generate energetic electron-hole pairs, called *hot carriers*, that are of great interest in photocatalytic processes and conversion of light into electric current for photodetection and photovoltaic applications.^{110,111} From this perspective, small nanoparticles (diameters below 20 nm) where absorption cross section is much larger than both scattering and geometrical cross sections, represent ideal systems for the efficient photon to hot-carriers conversion. After the typical lifetime of a plasmon excitation (~ 10 fs), hot electron-hole pairs are created giving rise to a non-equilibrium distribution of electrons (holes) with energy above (below) the Fermi energy.¹¹²

Experimental investigations showed that the timescale of the hot carriers generation has lifetimes in the range of 0.05-1 ps, depending on the material composition.^{113,114} The lifetime and particle size play a crucial role in determine the number of carrier generated with high energy (Fig. 5a-b). In large nanoparticles the density of states increases towards the continuum, providing an increasing number of available states at low energies (around the Fermi level). On the other hand, the reduction of the carrier lifetime defines the time-range where a non-equilibrium distribution of hot carriers exists before thermalization via electron-electron and electron-phonon interactions.¹¹³

The particle shape is also affecting the generation process. The hot carriers energy distribution δN was found proportional to the field enhancement factor κ inside the particle as follow¹¹⁵

$$\delta N \propto \frac{|\kappa(\omega)|^2}{\omega^4} \quad (5)$$

Since $\kappa(\omega)$ follows the behavior of the polarizability, equation (5) shows that the maximum density of hot carriers is obtained in correspondence of the plasmonic resonance where the absorption cross section reaches the maximum. Moreover, because κ is shape-dependent also the hot carrier generation results affected. Figure 5c compares field enhancement factors for a metal slab, a sphere, a cube and an ellipsoid, showing that among these geometries the ellipsoid is expected to be more efficient in creating hot electron-hole pairs.

While metal nanoparticles can be used as active elements to convert incident radiation into electron-holes with energy up to the plasmon quanta $\hbar\omega_p$, an interface with another object, for instance a semiconductor, is required to extract the hot carriers from the metal before they relax down to the ground state (see Fig. 5d). Carriers injection however, introduces an additional limitation to the overall process efficiency. Typical Schottky barrier heights (Φ_b) at the metal-semiconductor in-

terface are in the range of 0.5-1 eV, therefore electrons with energy below Φ_b have an exponentially decreasing probability to be injected. In surface plasmon polaritons, launched at a metal/semiconductor interface, the conservation of the momentum allows to increase each carrier energy by $\sim \hbar q v_f$, giving rise to a large number of carriers having a sharp distribution near the Fermi energy.¹¹² However, for SPP wavelength in the visible range (500-700 nm) $\hbar q v_f$ is on the order of ~ 10 meV, much below Φ_b . On the other hand, in metal nanostructures, since the momentum is not conserved due to the scattering with the surface, the energy conservation allows excitation of single carriers up to the maximum available energy $\hbar\omega_p$, that in the visible range is 1.5-2 eV, above Φ_b . This simple argument shows the importance of size reduction and corroborates the use of metal nanoparticles for hot-carrier generation. However, energy larger than the interface barrier is not the only requirement for the carrier injection. At an ideal flat interface, the conservation of the momentum parallel to the interface \mathbf{P}_\perp imposes that only carriers having

$$\frac{\mathbf{P}_\perp^2}{2m} \geq E_F + \Phi_b \quad (6)$$

are allowed to cross the border. Consequently, in a perfect metal-semiconductor junction, the electron injection rate can be well approximated by the Fowler equation¹¹⁶

$$I_{ph} = I_0 \cdot (\hbar\omega - \Phi_b)^2 \quad (7)$$

where $\hbar\omega$ is the energy of the incident radiation and Φ_b the barrier height at the interface. Finally, once the hot carriers are in the semiconductor, they need to be efficiently collected via an external applied circuit therefore the semiconductor materials with high mobility and device architecture with short collection paths play a crucial role to increase the overall process efficiency.

In conclusion, metal nanoparticles with large absorption cross section represent a quasi-ideal system to convert electromagnetic radiation into electric current. A number of parameters such as particle shape, size, carrier lifetime affect the hot carrier generation efficiency and optimized injection and carrier collection schemes need to be designed to exploit this process in real devices. In this contest, HbNW-based architectures afford a number of advantages compared to traditional 2D planar geometries that will be discussed in section 4.

4 Hybrid nanostructures: Applications

4.1 Optoelectronic applications

The optical and electronic properties of individual semiconductor nanowires and metal nanoparticles discussed in section 3 naturally make optoelectronic one of the most exciting fields of applications for HbNW nanostructures. In fact

hybrid architectures afford the promise to combine expanded capabilities, higher performances and miniaturization of optoelectronic devices thus increasing device efficiency, speed and reducing power consumption.

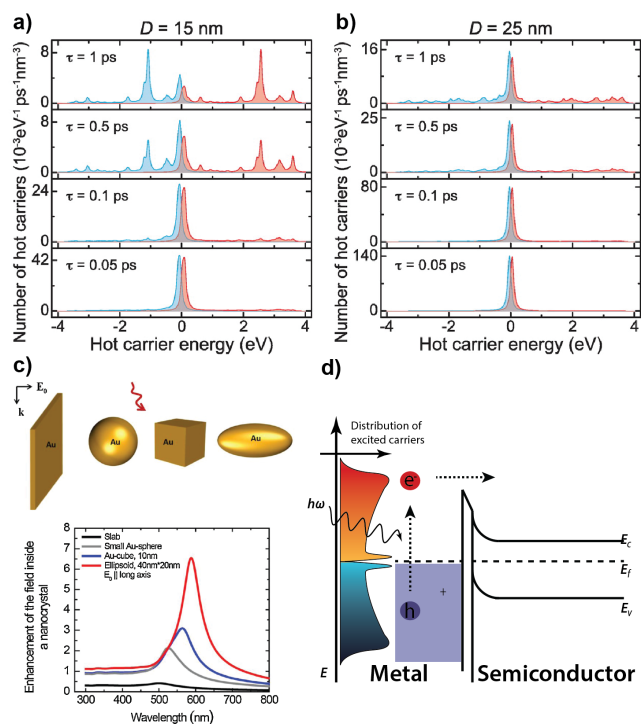


Fig. 5 Distribution of hot electrons (red lines) and hot holes (blue lines) generated per unit of time and volume as a function of their energy respect to the Fermi level. The plots compare four different hot carrier lifetimes τ ranging from 0.05 to 1 ps and nanoparticle diameters of a) 15 nm, and b) 25 nm.¹¹³ In the particle with diameter 15 nm the carrier distribution was found extending across the all interval of energies. A decrease in the lifetime results in a narrower distribution near the Fermi energy with a larger number of excited particles. A similar trend was also observed by increasing the diameter to 25 nm. c) Simulated enhancement factor in metal nanoparticles with different shapes showing that the ellipsoidal geometry is the most advantageous.¹¹² d) Schematic representation of the hot electron generation and injection process at a metal-semiconductor interface. Adapted with permission from a)-b) Copyright 2014, ACS; c) Copyright 2010, Elsevier

In particular, the fields of photodetection and photovoltaics could largely benefit from the enhanced properties of HbNWs. In traditional 2D semiconductor devices, the minimum lateral size and thicknesses of the active region are determined by the diffraction-limited spot size of light and the characteristic absorption depth of the material. These constraints limit the device miniaturization to the size range of microns. Also, strong carrier recombination in an active region with dimen-

sions much larger than the carrier mean free path penalizes device performances.⁶⁴ Semiconductor nanowires address some of these limitations by means of nanoscale dimensions and faster carrier collection due to shorter transit paths. However, reduced dimensions below the characteristic absorption depth prevent efficient light trapping thus limiting the overall efficiency.¹¹⁷ Integration of metallic nanostructures to enhance light absorption by the intensified local electric field, represents a viable pathway to improve the performance of both photodetectors and solar cell nanowire-based devices. For instance, near-field coupling between plasmonic nanostructures in proximity of a GaAs nanowire was used to redirect the electromagnetic radiation and enhancing up to 20 times the intensity into the semiconductor for determined wavelength and polarization, allowing to tailor the nonlinear optical response of a single nanowire.³⁰ Enhancement of second harmonic generation by ~ 1700 times was reported by Grimblat *et al.* for ZnO nanowire placed in the electric field hot-spot generated by gold pentamer oligomer.¹¹⁸ The coupling between leaky mode resonances (LMR) in nanowires and localized surface plasmons has been also investigated. In a bare semiconductor nanowire, LMRs represent the electromagnetic modes supported by the dielectric cavity where the absorption is resonantly enhanced.⁵⁹ The leaky nature of these modes facilitated their interaction with the surface plasmons of metal nanostructures on the nanowire surface. The resulting coupling allowed to suppress, enhance and shift the absorption resonances, expanding largely the level of control in tunability and modulation of the optical properties.^{29,119}

Different proof-of-concept hybrid nanowire photodetectors have been designed based on the enhanced light absorption in hybrid nanostructures.¹²⁰ For example Tang *et al.* exploited a dipole antenna to concentrate near-infrared radiation ($\sim 1.3 \mu\text{m}$) in metal-semiconductor-metal Ge photodetectors with sub-wavelength volume of the order of $10^{-4}\lambda^3$, demonstrating a plasmonic enhancement factor of 20 in the detected photocurrent.¹²¹ Hyun *et al.* used scanning photocurrent microscopy to resolve a local photocurrent enhancement by 20% along a Si nanowire decorated with Au nanoparticles under transverse polarization (Fig. 6a).³⁷ Reducing the gap separation between metal particles and Si nanowire down to the sub-nanometer range via galvanic displacement afforded a larger coupling with the plasmonic resonances, resulting in an enhanced photocurrent by a factor 2 compared to the bare nanowires. In addition, 5 time larger sensitivity and wavelength-dependent response was achieved by embedding Au nanoparticles inside the Si nanowire.^{33,122} Even larger boost in performance was found in Au-cluster-decorated InAs nanowire near-infrared photodetectors with a 3-folds enhancement in the responsivity compared to bare nanowire;¹²³ ZnO nanowires covered with Au nanoparticles also displayed an impressive 3 orders of magnitude enhanced on/off current ra-

tio and ~ 30 times faster recovery time compared to their bare counterparts.¹²⁴ Lu *et al.* investigated the UV photoresponse of ZnO nanorod arrays decorated with Al nanoparticles.¹²⁵ The lower ohmic losses of Al compared to other metals in the UV range naturally makes it a more suitable plasmonic material for hybrid UV photodetectors. The overall effect of the Al particles on the ZnO surface was a 12 times enhancement of the responsivity and a 6-fold increase of the on/off ratio. Result of the plasmonic activity of Al nanoparticles was also observed in the enhancement of the near-band edge emission and in a faster photoluminescence decay that was attributed to an effective coupling between the surface plasmons in metal particles and excitons in ZnO nanorods.¹²⁶ Metal particles on the nanowire surface can also induce oscillation of the photocurrent intensity as a function of the nanowire diameter due to the coupling of the surface plasmon with the allowed electromagnetic modes of the nanowire.¹²⁷ Luo *et al.* demonstrated a considerably improvement in the photodetection performance of CdSe nanoribbons decorated with Au hollow nanoparticle compared to bare CdSe nanoribbons and nanoribbons decorated with solid nanoparticles.¹²⁸ Furthermore, improved performance related to plasmonic enhanced light absorption was also observed in other hybrid systems including Au-decorated CdSe nanowires and CdTe nanowires,^{129,130} Au decorated ZnO/ZnCdSeTe core-shell nanowires,¹³¹ Ag decorated ZnO nanorod array LEDs,¹³² and Si nanowire arrays coated with Au nanoparticles decorated graphene film.¹³³

Knight *et al.* explored for the first time the alternative mechanism of hot-electron generation via plasmon decay for photodetection.¹³⁴ The proposed device, composed by an array of Au nanoantennas fabricated on an *n*-type Si substrate, showed a wavelength-resonant and polarization-sensitive photocurrent, demonstrating a spectral response at energies below the semiconductor bandgap with a quantum efficiency of $\sim 0.01\%$.¹³⁴ Recently, our group demonstrated this concept in Au nanorods-ZnO nanowire hybrid devices for near-infrared photodetection (Fig. 6b).⁴⁰ In the presented architecture, Au-nanorod-localized surface plasmons were used as active elements for generating and injecting hot electrons into the wide band gap ZnO nanowire, functioning as a passive component for charge collection. The hot electron generation and injection processes resulted in a large enhancement of the detected photocurrent at wavelengths where the ZnO nanowire was negligibly responsive on a time scale more than one order of magnitude faster than the typical ZnO photoresponse. Additionally, the quantum efficiency measured at the nanorod longitudinal plasmonic resonance (650 nm) was calculated to be approximately 3%, more than 30 times larger than values reported for hot-carrier based photodetectors with planar geometries,¹³⁵ thus demonstrating the advantage of using 1D hybrid architectures.

Other examples of enhanced capabilities in semiconduc-

tor devices integrated with plasmonic nanostructures can be found applied to solar cell technology. However, despite heterostructured nanowires represent a promising class of materials for solar cell devices,^{53,60,61,136–138} and the effectiveness in enhancing solar energy conversion via hybridization with metal nanoparticle was extensively demonstrated in thin-film solar cells,^{139–145} the investigation of HbNW nanostructures for photovoltaics has been still scarcely pursued.

Nevertheless, some remarkable examples in literature have shown that hybrid nanostructures have the potential to substantially improve different solar energy conversion systems. For instance, in Si nanowire/organic hybrid solar cells introduction of Ag nanoparticles on the nanowire surface resulted in a $\sim 30\%$ increasing in conversion efficiency and almost a 50% in the external quantum efficiency in the wavelength range 400–600 nm due to the nanoparticle-mediated absorption enhancement within the active polymer.¹⁴⁶ Decoration of ZnO nanowire arrays with Au nanoparticles in dye-sensitized solar cells allowed to exploit the advantages of the plasmonic-enhanced absorption and hot-carrier generation of metal nanoparticles with the reduced charges recombination due to the Schottky barrier at the Au-ZnO interface.¹⁴⁷ Kawawaki *et al.* improved the absorption of PbS QD/ZnO nanowire solar cells in the near-infrared range by including Ag nanocubes with an overall enhancement of the power conversion efficiency from 4.5% to 6%.¹⁴⁸ Within the solid-state p-n energy conversion scheme, core-shell silicon nanowire solar cells decorated with single silver nanocrystals showed wavelength-dependent enhancement of the short-circuit current (i.e. absorption) arising from both the near-field and far-field coupling with dipolar and quadrupolar nanocrystal resonances (Fig. 6c).¹⁴⁹ In solar to chemical energy conversion, plasmonic nanostructures deposited on semiconductor nanowire arrays have been also shown to enhance water splitting in the UV and visible regions of the spectrum via expanding and improving the absorption range of the bare nanowire arrays.^{150,151}

Finally, we mention that also the lasing properties of nanowires discussed in section 3.1 are affected by the presence of metal nanoparticles. Zhang *et al.* were the first to investigate the interaction between the plasmonic resonance of a spherical Ag nanoparticle and the Fabry-Perot modes in an optically pumped CdS nanowire. The wavelength and the relative intensity of resonance modes in the nanowire cavity were modulated by adjusting the particle position along the nanowire resulting in an enhancement of the cavity Q-factor of 56%.¹⁵²

4.2 Sensing applications

Another mechanism that can be explored and implemented in hybrid structures is surface-enhanced Raman spectroscopy

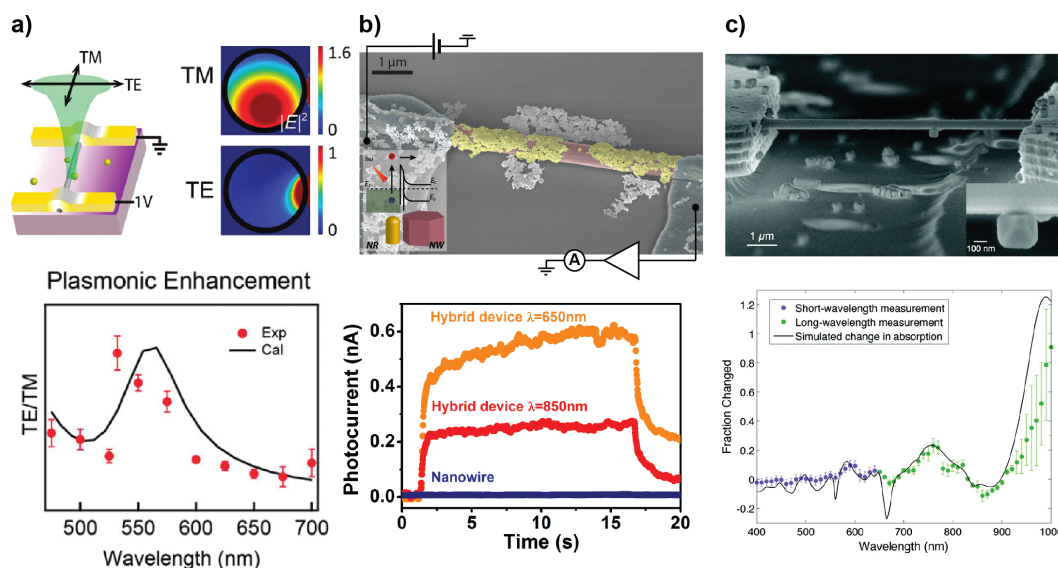


Fig. 6 a) Schematic of a HbNW photodetector and FDTD simulation of the field enhancement at the metal nanoparticle-nanowire interface (top). Enhancement of the ratio between photocurrent intensity under transversal and longitudinal polarization (bottom).³⁷ b) SEM image of the Au nanorods-decorated ZnO nanowire and schematic of the external applied circuit (top). The false colors highlight the different device components: ZnO nanowire (blue), Au nanorods (red), Ti/Al contacts (green). Comparison between the photocurrent spectra under light wavelength longer than 650 nm of a hybrid device and a bare ZnO nanowire (bottom).⁴⁰ c) SEM image of a single silicon nanowire solar cell decorated with an Ag octahedron and (bottom) the changes in photocurrent respect to the non decorated nanowire.¹⁴⁹ Adapted with permission from a) Copyright 2010, ACS; b) Copyright 2014, ACS; c) Copyright 2011, ACS;

(SERS). Raman scattering signals of single or few molecules adsorbed at or in proximity of metal nanostructures have been observed due to the many orders of magnitude plasmonic-mediated signal enhancement.¹⁵³ This approach, that expands the capability of traditional Raman spectroscopy, has become a widely explored technique to study molecular structures and to detect ultra-low concentration of molecules in sensing devices.^{154–156} In order to exploit and integrate these capabilities in real sensing devices, optimized fabrication techniques for SERS templates are required to maximize the sensitivity and avoid non-uniform distribution of nanoparticles that would result in poor reproducibility. Vertical arrays or *spaghetti-like* ensembles of nanowires decorated with metal nanoparticle represent an ideal candidate to achieve these requirements. The larger available surface provided by the nanowires compared to a flat surface allows an increasing of the nanoparticle density, i.e. field-enhanced hot spots, loaded on the substrate, thus resulting in a dramatic enhancement of the Raman signals by 6–7 orders of magnitude and low detection limits down to few hundreds ppms (Fig. 7a–b).^{47,48,157,158} Moreover, the decoration techniques are capable to realize an homogeneous distribution of nanoparticles over the entire substrate resulting in an excellent reproducibility of the results.^{159–161}

Additionally, SERS activity of metal nanostructures attached on the nanowire surface can also be exploited to

enhance the Raman scattering of the nanowire. For instance, metal nanoparticle decorated Si nanowires with sub-nanometer particle-nanowire gap separation led to an enhancement of the Raman signal up to a factor 28, recorded where two nanoparticles were found on either side of the nanowire (Fig. 7c–e).^{33,162} This approach provided an elegant way to perform in-situ resonant and non-resonant Raman spectroscopy investigation of homogeneous and heterostructured nanowires as well as characterization of nanowire surface optical phonon modes.¹⁶³

The sensitivity of the plasmonic resonance frequencies to the dielectric constant of the surrounding medium (see section 3.2.1) offers an alternative method of molecular recognition. The appearance of a target analyte in solution or its binding on a pre-functionalized nanoparticle metal surface modifies the medium permittivity and can be revealed via monitoring the frequency shift of the plasmonic resonances. This principle, previously demonstrated in 2D and 3D nanoparticle assemblies^{164–167} and other plasmonic structures,^{168–171} was recently demonstrated by Convertino *et al.* in silica nanowire forests decorated with Au and Ag nanoparticles where the light trapping effect in the nanowire ensemble resulted in a refractive index sensitivity among the highest reported in literature.¹⁷²

In the detection schemes previously described, metal

nanoparticles played the role of active elements while nanowires had mainly the function of a passive template. However, it should be mentioned that alternative detection strategies can be explored in HbNW-based sensors. Many proof-of-concept devices have been demonstrated able to detect ultra-low concentration of molecules either in gas phase or in solution using the properties of metal-semiconductor interface. As discussed in section 3.1, the advantages of using semiconductor nanowires for sensing rely on the high surface to volume ratio, providing high sensitivity, and on the gating effect of absorbed molecules on the channel conductivity, that allows a direct electrical readout of their concentrations.¹⁷³ Based on these properties, many authors demonstrated enhanced capabilities of HbNWs compared to pristine nanowires due to the combined gating and catalytic action carried out by the metal particles on the nanowire surface. In fact, for large enough densities of metal nanoparticles on the nanowire surface the Schottky barrier at the metal-semiconductor interface strongly affects the nanowire conductivity, conferring enhanced sensitivity to the surrounding medium.^{174–176} Additionally, metal nanoparticles own well-known catalytic properties (also affected by the plasmonic-mediated hot-carriers generation process)^{177–181} that allows a larger adsorption of molecules on the nanowire surface as well as a faster absorption/desorption process, thus enhancing the overall detection response of the hybrid nanostructures versus the bare nanowire.^{23,175,182–188}

The expanded capabilities of HbNWs are not limited to the enhanced detection sensitivity. Recently, schemes to improve the selectivity of the device response have been also proposed. Zou *et al.* showed the successful use of a metal nanoparticle decorated nanowire hybrid field-effect transistor as high selective gas sensor. In this prototype the engineered electronic properties of an In₂O₃ nanowire by Mg-doping, assisted by the catalytic properties of various metal particles, resulted in high sensitivity and selectivity in detecting CO, O₂, H₂ and C₂H₅OH.¹⁸⁹ An other important advantage offered by hybrid nanostructures is that metal nanoparticle surfaces can be easily functionalized in order to reach a selective response to target molecules in solutions. Pachauri *et al.* showed the feasibility of this approach demonstrating an ion-sensitive metal-semiconductor field-effect transistor for chemical sensing.¹⁹⁰

Overall, sensing represents one of the most promising and explored application for HbNW nanostructures. The possibility of exploiting and optimizing the entire capabilities, ranging from the plasmonic and catalytic properties of metal nanoparticle combined with the electrical transport in nanowires, represents an attractive prospective for developing the next generation of miniaturized sensors.

5 Conclusions and outlook

This brief snapshot on some of the most remarkable achievements obtained in the field of metal nanoparticle-semiconductor nanowire hybrid devices supports the high expectations and promises to solve key weaknesses of present technology in many fields. However, despite their great potential, HbNW nanostructures are not exempt from limitations and challenges to be addressed originating from both plasmonic and semiconductor nanowire components.

In plasmon-related processes the main limitation arises from the ohmic losses due to intraband and interband electronic transitions, described by a non-vanishing imaginary part of the permittivity ϵ'' in metals. Although the ideal case of $\epsilon''=0$ is not possible, every metal has an optimum optical region where the imaginary part reaches the minimum. For instance Au shows minimum losses for wavelength in the range 600–800 nm.¹⁹¹ At present, Au and Ag are the most used metals in plasmonic devices, as they also have the lowest ohmic losses. However, the large cost, especially of Au, has encouraged research of alternative low-cost materials,¹⁹² such as copper,^{193,194} aluminum¹⁹⁵ and alkali metals.¹⁹⁶ Alternative strategies in material engineering include growth of metallic compounds to obtain materials with reduced carrier concentration and consequently lower ohmic losses¹⁹⁷ and highly doped semiconductor with metallic-like behavior.¹⁹¹ However, investigation of these alternative materials in hybrid nanostructures is still lacking in literature.

On the semiconductor nanowire side, although the Vapor-Liquid-Solid growth conducted via different methods such as chemical vapor deposition, metal-organic chemical vapor deposition, molecular beam epitaxy, metal-organic vapor phase epitaxy and pulsed laser ablation methods,^{81,198,199} allows an outstanding control on the chemical composition, the synthesis of high-crystal quality materials requires expensive equipment. The associated scaling up of the growth process is also an issue that needs to be addressed in terms of cost and technological capabilities. Additionally, manipulation of these nanostructures and assembly in precise configurations represent an important limitation to the realization of integrated circuits based on nanowire elements, even though many different approaches ranging from self-assembly methods to nanopatterning^{200–203} have opened up viable routes for industrial-oriented applications.²⁰⁴

Overall, fabrication of metal nanostructures by design on the nanowire surface, or in its proximity, actually represent the main limiting factor that hampers the fundamental investigation of these fascinating hybrid materials and remains one of the major bottlenecks for mass production of plasmonic hybrid devices. In fact, exploration of the properties of hybrid architectures is still at its infancy and more research needs to be done to explore new material combinations, geometry and

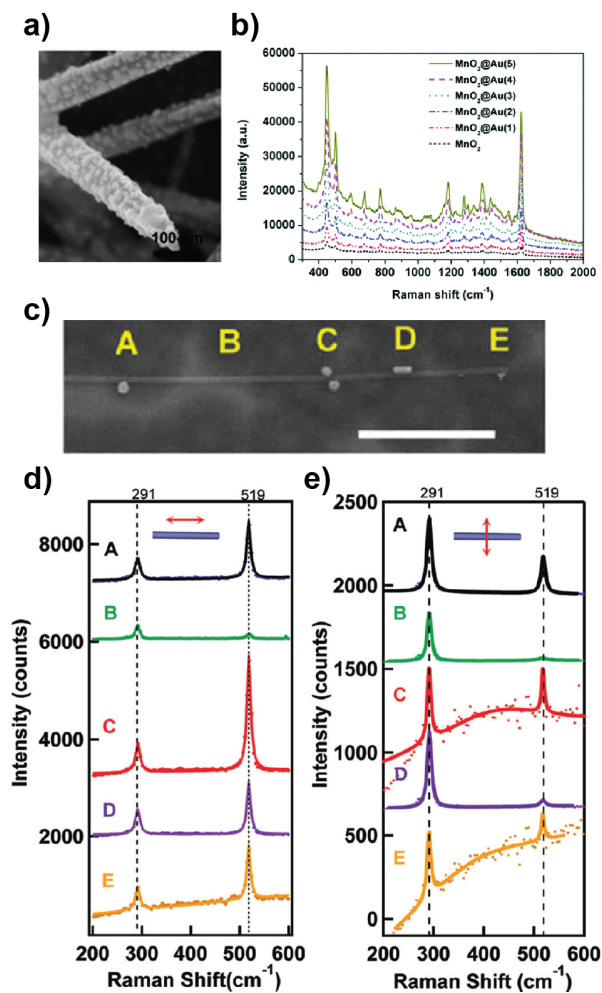


Fig. 7 HbNW for SERS applications. a) SEM image of the Au nanoparticle-coated MnO_2 nanowire and b) Raman scattering of methylene blue on MnO_2 nanowires covered by different amount of Au nanoparticles.⁴⁸ c) SEM image of a Si nanowire decorated with different Au nanostructures and Raman spectra recorded at different position along the nanowire with d) parallel and e) perpendicular polarization respect to the nanowire long axis.³³ Adapted with permission from a)-b) Copyright 2015, RSC; c)-e) Copyright 2012, ACS;

device capabilities. From the industrialization point of view, even though resolution of silicon manufacturing processes is actually capable to fabricate structures with nanometer dimension on the order of ~ 10 nm, realization of metal nanostructures requires alternative processes.¹⁹² From this perspective the use of highly doped semiconductors would facilitate the integration of plasmonic nanostructures in the present semiconductor-device technology by exploitation of CMOS-compatible strategies. On the other hand chemical synthesis of metal nanostructures²⁰⁵ offers a low-cost, high yield throughput that could potentially match the requirements imposed by industrial manufacturing but suffers from limited control on the nanowire decoration process and still requires further improvements for the fabrication of devices on large scale.

Nevertheless, the field of plasmonic-enhanced hybrid devices can be appointed as one of the most promising fields of research with potential large impact on future technological developments. The promising results obtained so far are strongly driving increasing scientific efforts in further development, optimization and integration of plasmonic devices with present electronic components, towards a new chip-scale technology taking advantage from the strengths of both plasmonic and electronic components.

Acknowledgements

This work was supported by the European Commission under FP7 ITN project Nanowiring (265073) and by FP7 NMP project Hysens (263091).

References

- 1 T. D. Ladd, F. Jelezko, R. Laflamme, Y. Nakamura, C. Monroe and J. L. O'Brien, *Nature*, 2010, **464**, 45–53.
- 2 M. L. Brongersma and V. M. Shalaev, *Science*, 2010, **328**, 440–441.
- 3 R. Zia, J. A. Schuller, A. Chandran and M. L. Brongersma, *Materials today*, 2006, **9**, 20–27.
- 4 D. K. Gramotnev and S. I. Bozhevolnyi, *Nature Photonics*, 2010, **4**, 83–91.
- 5 N. C. Lindquist, P. Nagpal, K. M. McPeak, D. J. Norris and S.-H. Oh, *Reports on progress in physics. Physical Society (Great Britain)*, 2012, **75**, 036501.
- 6 J. Schuller, E. Barnard, W. Cai, Y. Jun, J. White and M. Brongersma, *Nature materials*, 2010, **9**, 193–204.
- 7 P. Silvestroni, *Fondamenti di chimica*, Editoriale Veschi, 1989.
- 8 A. Polman and H. A. Atwater, *Materials today*, 2005, **8**, 56.
- 9 W. L. Barnes, A. Dereux and T. W. Ebbesen, *Nature*, 2003, **424**, 824–830.

- 10 S. A. Maier, M. L. Brongersma, P. G. Kik, S. Meltzer, A. A. G. Requicha and H. A. Atwater, *Advanced Materials*, 2001, **13**, 1501–1505.
- 11 H. Cang, A. Labno, C. Lu, X. Yin, M. Liu, C. Gladden, Y. Liu and X. Zhang, *Nature*, 2011, **469**, 385–388.
- 12 N. Liu, M. Tang, M. Hentschel, H. Giessen and A. Alivisatos, *Nature materials*, 2011, **10**, 631–636.
- 13 K. Mølhave, B. A. Wacaser, D. H. Petersen, J. B. Wagner, L. Samuelson and P. Bøggild, *small*, 2008, **4**, 1741–1746.
- 14 C. J. Barrelet, Y. Wu, D. C. Bell and C. M. Lieber, *Journal of the American Chemical Society*, 2003, **125**, 11498–11499.
- 15 P. V. Radovanovic, C. J. Barrelet, S. Gradecak, F. Qian and C. M. Lieber, *Nano letters*, 2005, **5**, 1407–1411.
- 16 J. Johansson, L. S. Karlsson, C. P. T. Svensson, T. Mårtensson, B. A. Wacaser, K. Deppert, L. Samuelson and W. Seifert, *Nature materials*, 2006, **5**, 574–580.
- 17 E. Ertekin, P. A. Greaney, D. C. Chrzan and T. D. Sands, *Journal of Applied Physics*, 2005, **97**, 114325.
- 18 C. Cheng, E. Sie, B. Liu, C. Huan, T. Sum, H. Sun and H. Fan, *Applied Physics Letters*, 2010, **96**, 071107.
- 19 J. K. Hyun and L. J. Lauhon, *Nano letters*, 2011, **11**, 2731–2734.
- 20 R. Chen, D. Li, H. Hu, Y. Zhao, Y. Wang, N. Wong, S. Wang, Y. Zhang, J. Hu, Z. Shen *et al.*, *The Journal of Physical Chemistry C*, 2012, **116**, 4416–4422.
- 21 S. Dhara and P. Giri, *Journal of Applied Physics*, 2011, **110**, 124317–9.
- 22 Y. J. Fang, J. Sha, Z. L. Wang, Y. T. Wan, W. W. Xia and Y. W. Wang, *Behind the change of the photoluminescence property of metal-coated ZnO nanowire arrays*, *Appl. Phys. Lett.*, 2011, vol. 98, p. 033103.
- 23 A. Kolmakov, D. Klenov, Y. Lilach, S. Stemmer and M. Moskovits, *Nano Letters*, 2005, **5**, 667–673.
- 24 Y. Hatakeyama, T. Morita, S. Takahashi, K. Onishi and K. Nishikawa, *The Journal of Physical Chemistry C*, 2011, **115**, 3279–3285.
- 25 N. P. Dasgupta, C. Liu, S. Andrews, F. B. Prinz and P. Yang, *Journal of the American Chemical Society*, 2013, **135**, 12932–12935.
- 26 S. T. Christensen, H. Feng, J. L. Libera, N. Guo, J. T. Miller, P. C. Stair and J. W. Elam, *Nano Letters*, 2010, **10**, 3047–3051.
- 27 N. P. Dasgupta, H. J. Jung, O. Trejo, M. T. McDowell, A. Hryciw, M. Brongersma, R. Sinclair and F. B. Prinz, *Nano Letters*, 2011, **11**, 934–940.
- 28 J. S. King, A. Wittstock, J. Biener, S. O. Kucheyev, Y. M. Wang, T. F. Baumann, S. K. Giri, A. V. Hamza, M. Baeumer and S. F. Bent, *Nano Letters*, 2008, **8**, 2405–2409.
- 29 C. Colombo, P. Krogstrup, J. Nygård, M. L. Brongersma and A. F. i Morral, *New Journal of Physics*, 2011, **13**, 123026.
- 30 A. Casadei, E. F. Pecora, J. Trevino, C. Forestiere, D. Ruffer, E. Russo-Averchi, F. Matteini, G. Tutuncuoglu, M. Heiss, A. Fontcuberta i Morral and L. Dal Negro, *Nano Letters*, 2014, **14**, 2271–2278.
- 31 J. A. Scholl, A. L. Koh and J. A. Dionne, *Nature*, 2012, **483**, 421–427.
- 32 N. J. Halas, S. Lal, W.-S. Chang, S. Link and P. Nordlander, *Chemical Reviews*, 2011, **111**, 3913–3961.
- 33 R. Chen, D. Li, H. Hu, Y. Zhao, Y. Wang, N. Wong, S. Wang, Y. Zhang, J. Hu, Z. Shen and Q. Xiong, *The Journal of Physical Chemistry C*, 2012, **116**, 4416–4422.
- 34 K.-Q. Peng, X. Wang, X.-L. Wu and S.-T. Lee, *Nano Letters*, 2009, **9**, 3704–3709.
- 35 C. Pacholski, A. Kornowski and H. Weller, *Angewandte Chemie International Edition*, 2004, **43**, 4774–4777.
- 36 G. Shen and D. Chen, *The Journal of Physical Chemistry C*, 2010, **114**, 21088–21093.
- 37 J. K. Hyun and L. J. Lauhon, *Nano Letters*, 2011, **11**, 2731–2734.
- 38 M. W. Knight, N. K. Grady, R. Bardhan, F. Hao, P. Nordlander and N. J. Halas, *Nano Letters*, 2007, **7**, 2346–2350.
- 39 R. D. Deegan, O. Bakajin, T. F. Dupont, G. Huber, S. R. Nagel and T. A. Witten, *Nature*, 1997, **389**, 827–829.
- 40 A. Pescaglini, A. Martín, D. Cammi, G. Juska, C. Ronning, E. Pelucchi and D. Iacopino, *Nano letters*, 2014, **14**, 6202–6209.
- 41 B. Nikoobakht and M. A. El-Sayed, *Chemistry of Materials*, 2003, **15**, 1957–1962.
- 42 N. R. Jana, L. Gearheart and C. J. Murphy, *The Journal of Physical Chemistry B*, 2001, **105**, 4065–4067.
- 43 A. A. Ashkarran and A. Bayat, *International Nano Letters*, 2013, **3**, 50.
- 44 E. C. Le Ru, J. Grand, I. Sow, W. R. Somerville, P. G. Etchegoin, M. Treguer-Delapierre, G. Charron, N. Félidj, G. Lévi and J. Aubard, *Nano letters*, 2011, **11**, 5013–5019.
- 45 C. Novo, A. M. Funston, I. Pastoriza-Santos, L. M. Liz-Marzan and P. Mulvaney, *The Journal of Physical Chemistry C*, 2007, **112**, 3–7.
- 46 X. Xia and Y. Xia, *Nano Letters*, 2012, **12**, 6038–6042.
- 47 R. Kattumenu, C. H. Lee, L. Tian, M. E. McConney and S. Singamaneni, *J. Mater. Chem.*, 2011, **21**, 15218–15223.
- 48 T. Jiang, L. Zhang, H. Jin, X. Wang and J. Zhou, *Dalton Transactions*, 2015, **44**, 7606–7612.
- 49 J.-P. Colinge, C.-W. Lee, A. Afzal, N. D. Akha-

- van, R. Yan, I. Ferain, P. Razavi, B. O'Neill, A. Blake, M. White *et al.*, *Nature nanotechnology*, 2010, **5**, 225–229.
- 50 M. A. Zimmler, D. Stichtenoth, C. Ronning, W. Yi, V. Narayanamurti, T. Voss and F. Capasso, *Nano letters*, 2008, **8**, 1695–1699.
- 57 J. Wang, M. S. Gudiksen, X. Duan, Y. Cui and C. M. Lieber, *Science*, 2001, **293**, 1455–1457.
- 58 C. Soci, A. Zhang, X.-Y. Bao, H. Kim, Y. Lo and D. Wang, *Journal of nanoscience and nanotechnology*, 2010, **10**, 1430–1449.
- 51 C. Soci, A. Zhang, B. Xiang, S. A. Dayeh, D. Aplin, J. Park, X. Bao, Y.-H. Lo and D. Wang, *Nano Letters*, 2007, **7**, 1003–1009.
- 52 L. Cao, J.-S. Park, P. Fan, B. Clemens and M. L. Brongersma, *Nano Letters*, 2010, **10**, 1229–1233.
- 59 L. Cao, J. S. White, J.-S. Park, J. A. Schuller, B. M. Clemens and M. L. Brongersma, *Nature materials*, 2009, **8**, 643–647.
- 60 E. C. Garnett, M. L. Brongersma, Y. Cui and M. D. McGehee, *Annual Review of Materials Research*, 2011, **41**, 269–295.
- 53 B. Tian, X. Zheng, T. J. Kempa, Y. Fang, N. Yu, G. Yu, J. Huang and C. M. Lieber, *Nature*, 2007, **449**, 885–889.
- 61 C. Colombo, M. Heiß, M. Gratzel and A. F. Morral, *Applied Physics Letters*, 2009, **94**, 173108–173108.
- 54 J. Wallentin, N. Anttu, D. Asoli, M. Huffman, I. Aberg, M. H. Magnusson, G. Siefert, P. Fuss-Kailuweit, F. Dimroth, B. Witzigmann, H. Q. Xu, L. Samuelson, K. Depert and M. T. Borgstrom, *science*, 2013, **339**, 1057–1060.
- 62 M. A. Green, K. Emery, Y. Hishikawa, W. Warta and E. D. Dunlop, *Progress in Photovoltaics: Research and Applications*, 2013, **21**, 1–11.
- 63 M. A. Green, *Physica E: Low-dimensional Systems and Nanostructures*, 2002, **14**, 65–70.
- 64 H. A. Atwater and A. Polman, *Nat Mater*, 2010, **9**, 205–213.
- 55 R. Roder, M. Wille, S. Geburt, J. Rensberg, M. Zhang, J. G. Lu, F. Capasso, R. Buschlinger, U. Peschel and C. Ronning, *Nano letters*, 2013, **13**, 3602–3606.
- 56 S. Chu, G. Wang, W. Zhou, Y. Lin, L. Chernyak, J. Zhao, J. Kong, L. Li, J. Ren and J. Liu, *Nat Nano*, 2011, **6**, 506–510.
- 65 J. C. Johnson, H. Yan, P. Yang and R. J. Saykally, *The Journal of Physical Chemistry B*, 2003, **107**, 8816–8828.
- 66 M. A. Zimmler, F. Capasso, S. Müller and C. Ronning, *Semiconductor Science and Technology*, 2010, **25**, 024001.
- 67 A. Pan, R. Liu, Q. Yang, Y. Zhu, G. Yang, B. Zou and K. Chen, *The Journal of Physical Chemistry B*, 2005, **109**, 24268–24272.
- 68 J. C. Johnson, H.-J. Choi, K. P. Knutsen, R. D. Schaller, P. Yang and R. J. Saykally, *Nature materials*, 2002, **1**, 106–110.
- 69 Y. Zhang, R. E. Russo and S. S. Mao, *Applied Physics Letters*, 2005, **87**, 043106.
- 70 F. Qian, Y. Li, S. Gradečak, H.-G. Park, Y. Dong, Y. Ding, Z. L. Wang and C. M. Lieber, *Nature materials*, 2008, **7**, 701–706.
- 71 F. Qian, S. Gradecak, Y. Li, C.-Y. Wen and C. M. Lieber, *Nano Letters*, 2005, **5**, 2287–2291.
- 72 S. Deshpande, T. Frost, L. Yan, S. Jahangir, A. Hazari, X. Liu, J. Mirecki-Millunchick, Z. Mi and P. Bhattacharya, *Nano Letters*, 2015, **15**, 1647–1653.
- 73 M. Heiss, Y. Fontana, A. Gustafsson, G. Wüst, C. Magen, D. O'Regan, J. Luo, B. Ketterer, S. Conesa-Boj, A. Kuhlmann *et al.*, *Nature materials*, 2013, **12**, 439–444.
- 74 N. Erhard, A. T. M. G. Sarwar, F. Yang, D. W. McComb, R. C. Myers and A. W. Holleitner, *Nano Letters*, 2015, **15**, 332–338.
- 75 Z. Yang, J. Xu, P. Wang, X. Zhuang, A. Pan and L. Tong, *Nano Letters*, 2011, **11**, 5085–5089.
- 76 A. Pan, W. Zhou, E. S. P. Leong, R. Liu, A. H. Chin, B. Zou and C. Z. Ning, *Nano Letters*, 2009, **9**, 784–788.
- 77 Z. Yang, D. Wang, C. Meng, Z. Wu, Y. Wang, Y. Ma, L. Dai, X. Liu, T. Hasan, X. Liu and Q. Yang, *Nano Letters*, 2014, **14**, 3153–3159.
- 78 J. Bao, M. A. Zimmler, F. Capasso, X. Wang and Z. F. Ren, *Nano Letters*, 2006, **6**, 1719–1722.
- 79 F. Qian, Y. Li, S. Gradecak, D. Wang, C. J. Barrelet and C. M. Lieber, *Nano letters*, 2004, **4**, 1975–1979.
- 80 M. H. Huang, S. Mao, H. Feick, H. Yan, Y. Wu, H. Kind, E. Weber, R. Russo and P. Yang, *science*, 2001, **292**, 1897–1899.
- 81 R. Yan, D. Gargas and P. Yang, *Nature Photonics*, 2009, **3**, 569–576.
- 82 S. R. Mahmoodi, B. Raissi, E. Marzbanrad, N. Shojayi, A. Aghaei and C. Zamani, *Procedia Chemistry*, 2009, **1**, 947–950.
- 83 N. Mohseni Kiasari and P. Servati, *Electron Device Letters, IEEE*, 2011, 1–3.
- 84 M.-W. Ahn, K.-S. Park, J.-H. Heo, D.-W. Kim, K. Choi and J.-G. Park, *Sensors and Actuators B: Chemical*, 2009, **138**, 168–173.
- 85 Q. Wan, Q. H. Li, Y. J. Chen, T. H. Wang, X. L. He, J. P. Li and C. L. Lin, *Applied Physics Letters*, 2004, **84**, 3654–3656.
- 86 L. Liao, H. B. Lu, J. C. Li, C. Liu, D. J. Fu and Y. L. Liu,

- Applied Physics Letters*, 2007, **91**, 173110–3.
- 87 J. Law and J. Thong, *Nanotechnology*, 2008, **19**, 205502.
- 88 R. Yu, C. Pan and Z. L. Wang, *Energy & Environmental Science*, 2013, **6**, 494–499.
- 89 Y. Han, C. Gao, H. Zhu, S. Chen, Q. Jiang, T. Li, M. Willander, X. Cao and N. Wang, *Nano Energy*, 2015, **13**, 405–413.
- 90 J. H. He and et al., *Nanotechnology*, 2009, **20**, 065503.
- 91 C. S. Lao, *Appl. Phys. Lett.*, 2007, **90**, 262107.
- 92 M. W. Ahn, K. S. Park, J. H. Heo, J. G. Park, D. W. Kim, K. J. Choi, J. H. Lee and S. H. Hong, *Applied Physics Letters*, 2008, **93**, 263103–3.
- 93 Y. Hu, J. Zhou, P.-H. Yeh, Z. Li, T.-Y. Wei and Z. L. Wang, *Advanced Materials*, 2010, **22**, 3327–3332.
- 94 P.-H. Yeh, Z. Li and Z. L. Wang, *Advanced Materials*, 2009, **21**, 4975–4978.
- 95 Y.-J. Choi, I.-S. Hwang, J.-G. Park, K. J. Choi, J.-H. Park and J.-H. Lee, *Nanotechnology*, 2008, **19**, 095508.
- 96 X. P. A. Gao, G. Zheng and C. M. Lieber, *Nano Letters*, 2009, **10**, 547–552.
- 97 P. Offermans, M. Crego-Calama and S. H. Brongersma, *Nano Letters*, 2010, **10**, 2412–2415.
- 98 E. Strelcov, Y. Lilach and A. Kolmakov, *Nano Letters*, 2009, **9**, 2322–2326.
- 99 S. Maier, *Plasmonics: fundamentals and applications*, Springer Verlag, 2007.
- 100 J. D. Jackson and J. D. Jackson, *Classical electrodynamics*, Wiley New York etc., 1962, vol. 3.
- 101 R. Gans, *Annalen der Physik*, 1912, **342**, 881–900.
- 102 C. F. Bohren and D. R. Huffman, *Absorption and Scattering of Light by Small Particles (Wiley science paperback series)*, Wiley-VCH, 1998.
- 103 K. L. Kelly, E. Coronado, L. L. Zhao and G. C. Schatz, *The Journal of Physical Chemistry B*, 2003, **107**, 668–677.
- 104 V. Sharma, K. Park and M. Srinivasarao, *Materials Science and Engineering: R: Reports*, 2009, **65**, 1–38.
- 105 F. J. Garcia de Abajo and A. Howie, *Phys. Rev. B*, 2002, **65**, 115418.
- 106 G. W. Bryant, F. J. Garcia de Abajo and J. Aizpurua, *Nano Letters*, 2008, **8**, 631–636.
- 107 K. S. Yee et al., *IEEE Trans. Antennas Propag*, 1966, **14**, 302–307.
- 108 E. C. Le Ru and P. G. Etchegoin, *MRS Bulletin*, 2013, **38**, 631–640.
- 109 A. O. Govorov and H. H. Richardson, *Nano Today*, 2007, **2**, 30–38.
- 110 C. Clavero, *Nat Photon*, 2014, **8**, 95–103.
- 111 M. L. Brongersma, N. J. Halas and P. Nordlander, *Nature nanotechnology*, 2015, **10**, 25–34.
- 112 A. O. Govorov, H. Zhang, H. V. Demir and Y. K. Gun'ko, *Nano Today*, 2014, **9**, 85–101.
- 113 A. Manjavacas, J. G. Liu, V. Kulkarni and P. Nordlander, *ACS nano*, 2014, **8**, 7630–7638.
- 114 S. Link and M. A. El-Sayed, *The Journal of Physical Chemistry B*, 1999, **103**, 8410–8426.
- 115 H. Zhang and A. O. Govorov, *The Journal of Physical Chemistry C*, 2014, **118**, 7606–7614.
- 116 R. H. Fowler, *Physical Review*, 1931, **38**, 45.
- 117 J. Lin, H. Li, H. Zhang and W. Chen, *Applied Physics Letters*, 2013, **102**, 203109–3.
- 118 G. Grinblat, M. Rahmani, E. Corts, M. Caldarola, D. Comedi, S. A. Maier and A. V. Bragas, *Nano Letters*, 2014, **14**, 6660–6665.
- 119 Y. Li, M. Li, D. Song, H. Liu, B. Jiang, F. Bai and L. Chu, *Nano Energy*, 2015, **11**, 756–764.
- 120 P. Berini, *Laser & Photonics Reviews*, 2014, **8**, 197–220.
- 121 L. Tang, S. E. Kocabas, S. Latif, A. K. Okyay, D.-S. Ly-Gagnon, K. C. Saraswat and D. A. Miller, *Nature Photonics*, 2008, **2**, 226–229.
- 122 M.-S. Hu, H.-L. Chen, C.-H. Shen, L.-S. Hong, B.-R. Huang, K.-H. Chen and L.-C. Chen, *Nat Mater*, 2006, **5**, 102–106.
- 123 J. Miao, W. Hu, N. Guo, Z. Lu, X. Zou, L. Liao, S. Shi, P. Chen, Z. Fan, J. C. Ho et al., *ACS nano*, 2014, **8**, 3628–3635.
- 124 K. Liu, M. Sakurai, M. Liao and M. Aono, *The Journal of Physical Chemistry C*, 2010, **114**, 19835–19839.
- 125 J. Lu, C. Xu, J. Dai, J. Li, Y. Wang, Y. Lin and P. Li, *Nanoscale*, 2015, **7**, 3396–3403.
- 126 J. Lu, J. Li, C. Xu, Y. Li, J. Dai, Y. Wang, Y. Lin and S. Wang, *ACS Applied Materials & Interfaces*, 2014, **6**, 18301–18305.
- 127 J. P. Sundararajan, P. Bakharev, I. Niraula, B. A. Fouetio Kengne, Q. MacPherson, M. Sargent, B. Hare and D. N. McIlroy, *Nano Letters*, 2012, **12**, 5181–5185.
- 128 L.-B. Luo, W.-J. Xie, Y.-F. Zou, Y.-Q. Yu, F.-X. Liang, Z.-J. Huang and K.-Y. Zhou, *Opt. Express*, 2015, **23**, 12979–12988.
- 129 R. Chakraborty, F. Greullet, C. George, D. Baranov, E. Di Fabrizio and R. Krahne, *Nanoscale*, 2013, **5**, 5334–5340.
- 130 L.-B. Luo, X.-L. Huang, M.-Z. Wang, C. Xie, C.-Y. Wu, J.-G. Hu, L. Wang and J.-A. Huang, *Small*, 2014, **10**, 2645–2652.
- 131 X. Zhan, Y. Bao, F. Wang, Q. Wang, Z. Cheng, Z. Wang, K. Xu, Z. Fang and J. He, *Applied Physics Letters*, 2015, **106**, 123904.
- 132 W. Z. Liu, H. Y. Xu, C. L. Wang, L. X. Zhang, C. Zhang, S. Y. Sun, J. G. Ma, X. T. Zhang, J. N. Wang and Y. C.

- Liu, *Nanoscale*, 2013, **5**, 8634–8639.
- 133 L.-B. Luo, L.-H. Zeng, C. Xie, Y.-Q. Yu, F.-X. Liang, C.-Y. Wu, L. Wang and J.-G. Hu, *Scientific reports*, 2014, **4**, 3914.
- 134 M. W. Knight, H. Sobhani, P. Nordlander and N. J. Halas, *Science*, 2011, **332**, 702–704.
- 135 M. W. Knight, Y. Wang, A. S. Urban, A. Sobhani, B. Y. Zheng, P. Nordlander and N. J. Halas, *Nano Letters*, 2013, **13**, 1687–1692.
- 136 B. Tian, T. J. Kempa and C. M. Lieber, *Chemical Society Reviews*, 2009, **38**, 16–24.
- 137 P. Krogstrup, H. I. Jørgensen, M. Heiss, O. Demichel, J. V. Holm, M. Aagesen, J. Nygard and A. F. i Morral, *Nature Photonics*, 2013, **7**, 306–310.
- 138 T. J. Kempa, B. Tian, D. R. Kim, J. Hu, X. Zheng and C. M. Lieber, *Nano letters*, 2008, **8**, 3456–3460.
- 139 C. Hagglund, M. Zach, G. Petersson and B. Kasemo, *Applied Physics Letters*, 2008, **92**, 053110.
- 140 D. Derkacs, S. Lim, P. Matheu, W. Mar and E. Yu, *Applied Physics Letters*, 2006, **89**, 093103–093103.
- 141 P. Reineck, G. P. Lee, D. Brick, M. Karg, P. Mulvaney and U. Bach, *Advanced Materials*, 2012, **24**, 4750–4755.
- 142 W. Zhang, M. Saliba, S. D. Stranks, Y. Sun, X. Shi, U. Wiesner and H. J. Snaith, *Nano Letters*, 2013, **13**, 4505–4510.
- 143 D. Derkacs, W. Chen, P. Matheu, S. Lim, P. Yu and E. Yu, *Applied Physics Letters*, 2008, **93**, 091107.
- 144 C. Hagglund, M. Zach and B. Kasemo, *Applied Physics Letters*, 2008, **92**, 013113–3.
- 145 E. Wei, X. Li and W. C. Choy, *Scientific reports*, 2014, **4**, year.
- 146 K. Liu, S. Qu, X. Zhang, F. Tan and Z. Wang, *Nanoscale research letters*, 2013, **8**, 1–6.
- 147 Z. H. Chen, Y. B. Tang, C. P. Liu, Y. H. Leung, G. D. Yuan, L. M. Chen, Y. Q. Wang, I. Bello, J. A. Zapien, W. J. Zhang, C. S. Lee and S. T. Lee, *The Journal of Physical Chemistry C*, 2009, **113**, 13433–13437.
- 148 T. Kawawaki, H. Wang, T. Kubo, K. Saito, J. Nakazaki, H. Segawa and T. Tatsuma, *ACS Nano*, 2015, **9**, 4165–4172.
- 149 S. Brittan, H. Gao, E. C. Garnett and P. Yang, *Nano letters*, 2011, **11**, 5189–5195.
- 150 Y.-C. Pu, G. Wang, K.-D. Chang, Y. Ling, Y.-K. Lin, B. C. Fitzmorris, C.-M. Liu, X. Lu, Y. Tong, J. Z. Zhang, Y.-J. Hsu and Y. Li, *Nano Letters*, 2013, **13**, 3817–3823.
- 151 X. Wang, K.-Q. Peng, Y. Hu, F.-Q. Zhang, B. Hu, L. Li, M. Wang, X.-M. Meng and S.-T. Lee, *Nano Letters*, 2014, **14**, 18–23.
- 152 Q. Zhang, X.-Y. Shan, X. Feng, C.-X. Wang, Q.-Q. Wang, J.-F. Jia and Q.-K. Xue, *Nano Letters*, 2011, **11**, 4270–4274.
- 153 N. J. Halas and M. Moskovits, *MRS Bulletin*, 2013, **38**, 607–611.
- 154 B. Sharma, M. Fernanda Cardinal, S. L. Kleinman, N. G. Greeneltch, R. R. Frontiera, M. G. Blaber, G. C. Schatz and R. P. Van Duyne, *MRS Bulletin*, 2013, **38**, 615–624.
- 155 T. Chen, H. Wang, G. Chen, Y. Wang, Y. Feng, W. S. Teo, T. Wu and H. Chen, *Acs Nano*, 2010, **4**, 3087–3094.
- 156 R. F. Aroca, *Physical Chemistry Chemical Physics*, 2013, **15**, 5355–5363.
- 157 J.-A. Huang, Y.-Q. Zhao, X.-J. Zhang, L.-F. He, T.-L. Wong, Y.-S. Chui, W.-J. Zhang and S.-T. Lee, *Nano letters*, 2013, **13**, 5039–5045.
- 158 J. Chen, T. Mårtensson, K. A. Dick, K. Deppert, H. Xu, L. Samuelson and H. Xu, *Nanotechnology*, 2008, **19**, 275712.
- 159 B. Zhang, H. Wang, L. Lu, K. Ai, G. Zhang and X. Cheng, *Advanced Functional Materials*, 2008, **18**, 2348–2355.
- 160 M. Peng, J. Gao, P. Zhang, Y. Li, X. Sun and S.-T. Lee, *Chemistry of Materials*, 2011, **23**, 3296–3301.
- 161 H. He, W. Cai, Y. Lin and B. Chen, *Langmuir*, 2010, **26**, 8925–8932.
- 162 Z. Peng, H. Hu, M. I. B. Utama, L. M. Wong, K. Ghosh, R. Chen, S. Wang, Z. Shen and Q. Xiong, *Nano Letters*, 2010, **10**, 3940–3947.
- 163 A. Pescaglini, E. Secco, A. Martin, D. Cammi, C. Ronning, N. Garro and D. Iacopino, *in preparation*, 2015.
- 164 K. Sugawa, H. Tahara, A. Yamashita, J. Otsuki, T. Sagara, T. Harumoto and S. Yanagida, *ACS Nano*, 2015, **9**, 1895–1904.
- 165 J. Ye, K. Bonroy, D. Nelis, F. Frederix, J. Dhaen, G. Maes and G. Borghs, *Colloids and Surfaces A: Physicochemical and Engineering Aspects*, 2008, **321**, 313–317.
- 166 S. Zeng, K.-T. Yong, I. Roy, X.-Q. Dinh, X. Yu and F. Luan, *Plasmonics*, 2011, **6**, 491–506.
- 167 L. Guo, G. Chen and D.-H. Kim, *Analytical chemistry*, 2010, **82**, 5147–5153.
- 168 A. Kabashin, P. Evans, S. Pastkovsky, W. Hendren, G. Wurtz, R. Atkinson, R. Pollard, V. Podolskiy and A. Zayats, *Nature materials*, 2009, **8**, 867–871.
- 169 H. Chen, X. Kou, Z. Yang, W. Ni and J. Wang, *Langmuir*, 2008, **24**, 5233–5237.
- 170 Y. Shen, J. Zhou, T. Liu, Y. Tao, R. Jiang, M. Liu, G. Xiao, J. Zhu, Z.-K. Zhou, X. Wang *et al.*, *Nature communications*, 2013, **4**, year.
- 171 A. G. Brolo, *Nature Photonics*, 2012, **6**, 709–713.
- 172 A. Convertino, M. Cuscun, F. Martelli, M. G. Manera and R. Rella, *The Journal of Physical Chemistry C*, 2014,

- 118, 685–690.
- 173 P. Feng, F. Shao, Y. Shi and Q. Wan, *Sensors*, 2014, **14**, 17406–17429.
- 174 Y. Zhang, J. Xu, P. Xu, Y. Zhu, X. Chen and W. Yu, *Nanotechnology*, 2010, **21**, 285501.
- 175 C. Li, L. Li, Z. Du, H. Yu, Y. Xiang, Y. Li, Y. Cai and T. Wang, *Nanotechnology*, 2008, **19**, 035501.
- 176 J.-H. Ahn, J. Yun, Y.-K. Choi and I. Park, *Applied Physics Letters*, 2014, **104**, 013508.
- 177 K. Weidemaier, H. L. Tavernier and M. D. Fayer, *The Journal of Physical Chemistry B*, 1997, **101**, 9352–9361.
- 178 Z. Han, L. Wei, Z. Zhang, X. Zhang, H. Pan and J. Chen, *Plasmonics*, 2013, **8**, 1193–1202.
- 179 C. Hu, T. Peng, X. Hu, Y. Nie, X. Zhou, J. Qu and H. He, *Journal of the American Chemical Society*, 2009, **132**, 857–862.
- 180 F. Wu, X. Hu, J. Fan, E. Liu, T. Sun, L. Kang, W. Hou, C. Zhu and H. Liu, *Plasmonics*, 2013, **8**, 501–508.
- 181 K. T. Shimizu, R. A. Pala, J. D. Fabbri, M. L. Brongersma and N. A. Melosh, *Nano letters*, 2006, **6**, 2797–2803.
- 182 R. K. Joshi, Q. Hu, F. Alvi, N. Joshi and A. Kumar, *The Journal of Physical Chemistry C*, 2009, **113**, 16199–16202.
- 183 W. Lim, J. Wright, B. Gila, J. L. Johnson, A. Ural, T. Anderson, F. Ren and S. Pearton, *Applied Physics Letters*, 2008, **93**, 072109–072109.
- 184 V. Dobrokhotov, D. McIlroy, M. G. Norton, A. Abuzir, W. Yeh, I. Stevenson, R. Pouy, J. Bochenek, M. Cartwright, L. Wang *et al.*, *Journal of applied physics*, 2006, **99**, 104302.
- 185 V. Dobrokhotov, D. McIlroy, M. G. Norton, R. Abdelrahman, A. Safir and C. Berven, *Nanotechnology*, 2009, **20**, 135504.
- 186 J. Yun, C. Y. Jin, J.-H. Ahn, S. Jeon and I. Park, *Nanoscale*, 2013, **5**, 6851–6856.
- 187 W. Dong, H. Huang, Y. Zhu, X. Li, X. Wang, C. Li, B. Chen, G. Wang and Z. Shi, *Nanotechnology*, 2012, **23**, 425602.
- 188 N. Singh, R. K. Gupta and P. S. Lee, *ACS applied materials & interfaces*, 2011, **3**, 2246–2252.
- 189 X. Zou, J. Wang, X. Liu, C. Wang, Y. Jiang, Y. Wang, X. Xiao, J. C. Ho, J. Li, C. Jiang, Y. Fang, W. Liu and L. Liao, *Nano Letters*, 2013, **13**, 3287–3292.
- 190 V. Pachauri, K. Kern and K. Balasubramanian, *Applied Physics Letters*, 2013, **102**, 023501–5.
- 191 G. V. Naik, V. M. Shalaev and A. Boltasseva, *Advanced Materials*, 2013, **25**, 3264–3294.
- 192 C. L. Nathan, N. Prashant, M. M. Kevin, J. N. David and O. Sang-Hyun, *Reports on Progress in Physics*, 2012, **75**, 036501.
- 193 J. H. Kim, S. H. Ehrman and T. A. Germer, *Applied physics letters*, 2004, **84**, 1278–1280.
- 194 H. Gao, J. Henzie, M. H. Lee and T. W. Odom, *Proceedings of the National Academy of Sciences*, 2008, **105**, 20146–20151.
- 195 K. Ray, M. H. Chowdhury and J. R. Lakowicz, *Analytical chemistry*, 2007, **79**, 6480–6487.
- 196 M. D. Arnold and M. G. Blaber, *Optics express*, 2009, **17**, 3835–3847.
- 197 M. G. Blaber, M. D. Arnold and M. J. Ford, *Journal of Physics: Condensed Matter*, 2010, **22**, 143201.
- 198 S. R. Plissard, D. R. Slapak, M. A. Verheijen, M. Hocevar, G. W. Immink, I. van Weperen, S. Nadj-Perge, S. M. Frolov, L. P. Kouwenhoven and E. P. Bakkers, *Nano letters*, 2012, **12**, 1794–1798.
- 199 L. Chen, W. Lu and C. M. Lieber, *Semiconductor Nanowires: From Next-Generation Electronics to Sustainable Energy*, The Royal Society of Chemistry, 2015, pp. 1–53.
- 200 D. Whang, S. Jin and C. M. Lieber, *Nano Letters*, 2003, **3**, 951–954.
- 201 C. M. Lieber and Z. L. Wang, *Mrs Bulletin*, 2007, **32**, 99–108.
- 202 A. Javey, S. Nam, R. S. Friedman, H. Yan and C. M. Lieber, *Nano letters*, 2007, **7**, 773–777.
- 203 D. Whang, S. Jin, Y. Wu and C. M. Lieber, *Nano letters*, 2003, **3**, 1255–1259.
- 204 H. J. Fan, P. Werner and M. Zacharias, *small*, 2006, **2**, 700–717.
- 205 J. Perez-Juste, I. Pastoriza-Santos, L. M. Liz-Marzan and P. Mulvaney, *Coordination Chemistry Reviews*, 2005, **249**, 1870–1901.